ICOLD Symposium on Sustainable Development of Dams and River Basins, 24th - 27th February, 2021, New Delhi

PRACTICAL EVALUATION OF AAR-AFFECTED MACTAQUAC DAM

DAN D. CURTIS, LINGMIN (FRANK) FENG, GURINDERBIR S. SOOCH AND JIQIN (TOM) ZHENG
Hatch Ltd., Niagara Falls, Canada

IAN CAMPBELL
NB Power, Fredericton, Canada

ABSTRACT

Hatch has been involved in many hydro projects where alkali aggregate reaction (AAR) has affected dams and power plants. AAR causes the concrete to expand and this leads to issues including reduction in spillway and intake gate clearances, concrete cracking, high compressive and shear stresses in concrete substructures, stressing of turbine embedded parts and turbine/generator alignment problems. During the course of these investigations, a practical finite element program (GROW3D) has been developed to analyze the effects of concrete expansion on these structures. The program is based on relatively simple engineering principles yet it has proven to be a reliable tool in the prediction of the structural behavior of dams and power plants. The objective of this paper is to present selected results from recent analyses performed on the Mactaquac Dam and power plant which is located in New Brunswick, Canada. The stress-dependant concrete growth law used in GROW3D has recently been modified to better match the observed behavior of the Mactaquac intake structure response to slot cutting. The new concrete growth law was subsequently used in a global finite element analysis of the Mactaquac powerhouse and the results of the analysis provided an excellent match to measurements of structural and mechanical AAR-induced deformations. Finally, the powerful effect of differential concrete expansion in structural elements is examined using simple analytical methods.

1. INTRODUCTION

The Mactaquac Generating Station is located in New Brunswick, Canada, approximately 20 km upstream of the provincial capital of Fredericton on the St. John River. The station is the largest hydroelectric generating facility in the Maritime Provinces and was constructed in stages between 1964 and 1980.

The concrete of the structures are affected by alkali-aggregate reaction (AAR) in the specific form of alkali-silica reaction (ASR). This reaction causes the concrete to expand if unrestrained, or to develop large compressive forces, if restrained. Since 1985, various innovative remedial measures have been undertaken to mitigate the effects of concrete expansion on the structures and equipment. These have included various slots within the structures cut with a diamond wire saw, anchoring of structures, periodic grouting and modifications to existing gates and electro mechanical equipment. The concrete structures are monitored with an extensive instrumentation system. The concrete material properties are carefully monitored using a long-term testing program and periodic specialty testing. The design, analysis and implementation of remedial measures in the water retaining structures and powerhouse have been presented in other references, for example, Charlwood et al (1992), Thompson et al (1994), Curtis (1995) and Codrington et al (2007).

In 1985, Spillway Gate 10 was found to be jammed closed as a result of AAR-induced concrete expansion of the intake and spillway east end pier. In 1988, the first of several diamond wire slot cuts was installed between intake units as a means of controlling deformations. The initial finite element modeling predicted adverse intake water passage pier concrete cracking, and large post-tensioned anchors were installed to stabilize the structure if this cracking did occur. Slots were cut in the intake in 1988, 1989 and 1992. The slots were first cut with a 10-mm diamond wire saw. As concrete growth continues, periodic re-cutting of slots is required and most current cuts are made with a 15-mm diamond wire saw. The intake slots are cut periodically in order to prevent the ASR deformation from accumulating across the entire intake thus leading to large tilting of an intake block and/or the spillway east end pier (EEP) (as observed in 1985).

Figure 1 : Spillway Gates 6 to 10 are Left to Right; Intakes 1 to 6 from Right to Left

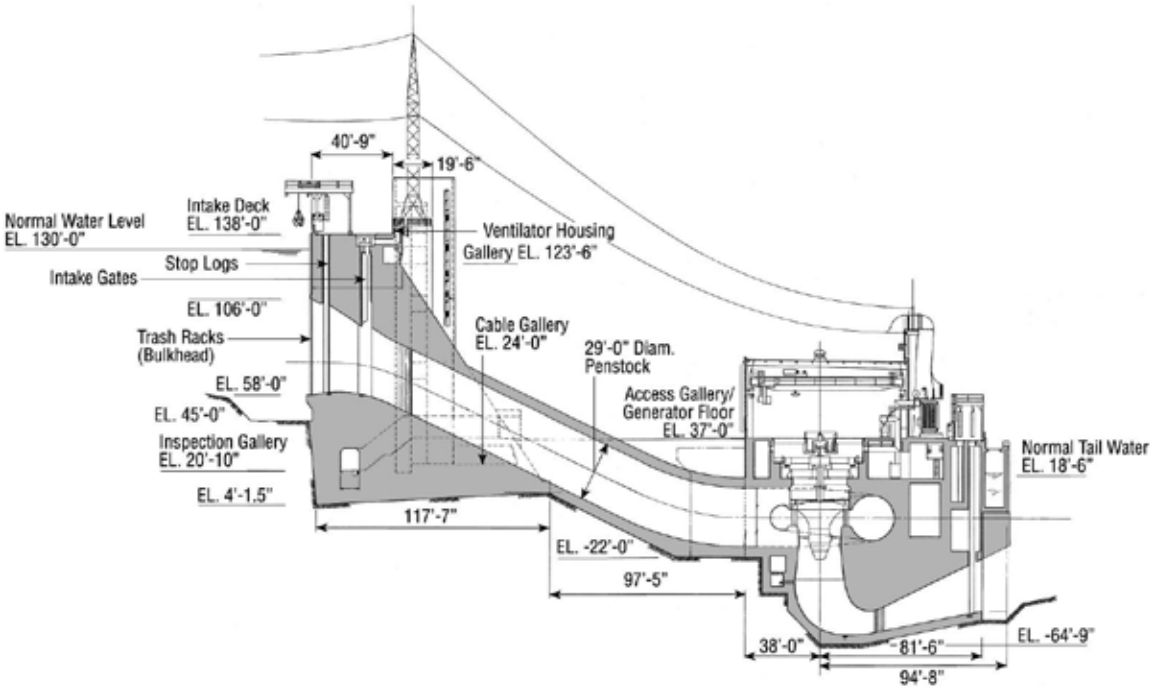

Figure 2 : Intake Section and Powerhouse

The powerhouse also suffers from AAR and the resulting expansion is causing turbine/generator alignment issues, development of large stresses in the turbine embedded part including the stay vanes, and large concrete stresses in the draft tube piers. In 1995, transverse slot cuts were installed in the unit block concrete between each unit of the powerhouse. In 1996, a program of cutting penstocks and installing couplings was initiated by working on one penstock per year. The cutting of the penstocks and installation of couplings allowed the upstream portion of the powerhouse to tilt upstream thereby reducing alignment issues, reducing stay vane stress buildup and reducing concrete stresses in the draft tube piers. The initial response to these remedial measures is described in Curtis (2001).

The short- and long-term deformation response of the intake and powerhouse is monitored with a large number of instruments including numerous extensometers, joint meters and inverted pendulums. The intake has inverted pendulums located on either side of the slots, a plumbline in the spillway EEP and invar rod extensometers running longitudinally in the upper galley (at el 123'-6" in Figure 2). The powerhouse has a similar set of instruments; however a very detailed monitoring program has also been established to monitor the turbine/generator movements. Further details can be found in Thompson et al (1995).

It must be recognized that the rates of concrete expansion at Mactaquac are in the range of 2 to 3 times larger than any other typical dam/power station affected by AAR. The maximum measured concrete growth rate is in the range of 130 to 150 micro-strain/year. As a result, the intake is almost 9 inches higher than originally constructed and the height of the intake gates had to be increased to accommodate this new dimension.

2. INCORPORATION OF CONCRETE GROWTH MATERIAL MODEL IN ANSYS

This section describes the important features of the GROW3D subroutines which Hatch has incorporated in ANSYS. The following is described:

- creep effects in AAR-affected concrete
- stress dependent concrete growth law
- temperature dependent concrete growth rate.

Creep Effects

The instantaneous strain occurring during the application of the stress is calculated by:

$$\varepsilon(t_o) = \frac{\sigma(t_o)}{E(t_o)} \quad ...(1)$$

Where

$\sigma(t_o)$ = the concrete stress at age t_o

$E(t_o)$ = the concrete modulus of elasticity at age to

t_o = the age of concrete at the time of loading.

Under sustained stress, concrete strain increases with time due to creep. The total strain – instantaneous plus creep – at time t is

$$\varepsilon_c(t, t_o) = \frac{\sigma(t_o)}{E(t)} \varphi(t, t_o) \quad ...(2)$$

Where

$\varphi(t,t_o)$ is the creep coefficient, which is a function of the age at loading, to, and the age t_o for which the strain is calculated. The creep coefficient φ represents the ratio of creep to the instantaneous strain.

$E(t)$ is the concrete modulus at time t.

Therefore, the creep strain under a constant stress is obtained by:

$$\varphi(t, t_o) = \frac{(t - t_o)^{0.6}}{10 + (t - t_o)^{0.6}} \varphi_\mu \quad ...(3)$$

For normal concrete, from Appendix A, Equation A.3.1 of Ghali and Favre (1994), the coefficient for creep at time t for age at loading t_o is given by:

$$\varphi(t, t_o) = \frac{(t - t_o)^{0.6}}{10 + (t - t_o)^{0.6}} \varphi_\mu \quad ...(4)$$

Where

φ_μ = the ultimate creep coefficient after a very long time (10,000 days) for age at loading, t_o

For $t–t_o$ = 5 years = 1,826.25 days

$$\varphi(t, t_o) = \frac{1826.25^{0.6}}{10 + 1826.25^{0.6}} = 0.90 \quad ...(5)$$

Therefore, 90% of the ultimate creep occurs in the first 5 years after the loading is applied.

φ_μ is a function of the characteristic compressive strength of concrete f_{ck}, the ambient relative humidity and average thickness of the member or its volume-to-surface ratio. Ghali and Favre (1994) provide graphs for $\varphi(t, t_o)$ with various f_{ck}, relative humidity and nominal size of the member. For dam structures, usually f_{ck} is low, the relative humidity is high and volume to-surface ratio is high. Therefore, Figure A.11 from Ghali and Favre (1994) with f_{ck} = 3,000 psi, RH=80% and nominal size h_o =40 inches is used for a mass concrete structure, i.e., the largest available size is used. From Figure A.11 of Ghali and Favre (1994), the φ_μ for various t_o is listed in Table 3.1-1 of Ghali and Favre (Table 1 below). When φ_μ versus log (t_o) is plotted, the three points are almost on a straight line. Therefore, φ_μ can be calculated from the following formula:

$$\varphi_\mu(t_o) = -0.4559 \times \log(t_o) + 1.222 \quad ...(6)$$

Where

t_o = the age of concrete at loading in unit of year.

Table 1 : Ultimate Creep Coefficient for Dam Structure

t_0 (day)	t_0 (year)	log10 (t_0) (year)	φ_μ
360	0.98562628	-0.006287724	1.227
700	1.91649555	0.282507815	1.089
1400	3.8329911	0.583537811	0.958

The stresses in an AAR affected concrete structure change with time as a result of continued concrete expansion. As indicated above, the creep strain is proportional to the applied stress. This linear relationship allows superposition of the creep strains due to stress changes. Therefore, when the magnitude of the applied stress changes with time, the total creep strain of concrete due to the applied stress is obtained by:

$$\varepsilon_c(t) = \frac{\sigma(t_o)}{E(t)}\varphi(t,t_o) + \int_{\sigma(t_o)}^{\sigma(t)} \frac{\varphi(t,\tau)}{E(t)} d\sigma(\tau) \qquad ...(7)$$

Where

t_o and t = the ages of concrete when the initial stress is applied and the strain is considered

τ = an intermediate age between to and t

$\sigma(t_o)$ = the initial stress applied at age t_o

$d\sigma(\tau)$ = the stress change applied at age τ

E(t) = the concrete modulus of elasticity at time t

$\varphi(t, t_o)$ = the creep coefficient at time t for loading at age t_o

$\varphi(t, \tau)$ = the creep coefficient at time t for loading at age τ.

In the AAR analysis using GROW3D, the time step is taken as one year. In order to calculate the creep strain, the six stress components at each gauss point of each element are saved as state variables in ANSYS. However, there is a limit on the number of time steps for which stresses can be stored due to limitations on computer resources. As indicated previously, over 90% of the ultimate creep strain occurs in the first five years after the stress is applied. Therefore, for practical purposes, only the stress components for the last five years preceding the current time step are saved for the calculation of creep strain.

AAR affected concrete has larger creep coefficient than normal concrete. To account for this, a factor CAAR is introduced which is the ratio of creep coefficient of AAR concrete over normal concrete. Thus, for AAR concrete, the creep coefficient is given by:

$$\varphi(t,t_o) = CAAR * \frac{(t-t_o)^{0.6}}{10+(t-t_o)^{0.6}} * \varphi_\mu \qquad ...(8)$$

By comparing the analysis results of AAR projects using the current nonlinear time dependent creep model with the previous linear time independent creep model, it is found that equivalent results are obtained with CAAR varying from 1.0 to 2.0.

2.1 Stress-Dependent Concrete Growth Law in ANSYS

The stress dependent concrete growth law is input to ANSYS using the user programmable features within ANSYS. It is noted that GROW3D was developed using measured displacements and concrete stresses from the Mactaquac Generating Station in New Brunswick, Canada. It was found that variation of concrete expansion strain rates with the log of stress provided a very good correlation with field measurements. In the field of rock mechanics dealing with swelling rocks, a similar relationship was found (as referenced in Curtis 1995).

The stress dependent growth law characterizing AAR-induced growth of concrete is given as follows:

$$\begin{aligned} \dot{\varepsilon}_{gi}(t) &= \dot{\varepsilon}_{g0}(t) && \text{for} \quad \bar{\sigma}_i < \sigma_0 \\ \dot{\varepsilon}_{gi}(t) &= \dot{\varepsilon}_{g0}(t) - K\left[log\left(\frac{\bar{\sigma}_i}{\sigma_0}\right)\right] && \text{for} \quad \sigma_0 < \bar{\sigma}_i < \sigma_{lim} \\ \dot{\varepsilon}_{gi}(t) &= 0 && \text{for} \quad \bar{\sigma}_i > \sigma_{lim} \end{aligned} \qquad ...(9)$$

Where

$\dot{\varepsilon}_{gi}(t)$ = concrete growth strains in principal directions at time (t)

$\dot{\varepsilon}_{g0}$ = unrestrained concrete growth rate at low stress at time (t)

K = slope of the line defining the concrete growth rate versus the log of stress

σ_i = the three principal stresses (i = 1 to 3)

σ_0 = a low compressive stress cut-off, whereby at lower compressive stresses or any tensile stress, the concrete growth rate is set at the unrestrained growth rate, and at larger compressive stresses, the concrete growth rate is reduced according to the above logarithmic growth law

σ_{lim} = the cut-off stress level beyond which no concrete expansion is assumed to occur.

At each time interval, the concrete growth strains are computed based on the previous stress state. The concrete growth strain increments are resolved in the direction of the principal stresses. These strain increments are the initial strain loads (internal loads) used in the finite element analysis of a given time step.

2.2 Temperature-Dependent Growth Rate

It is noted that GROW3D has been updated to include a temperature dependant concrete growth law and it has been used on other projects but currently not on Mactaquac. The temperature dependant growth law is important when calibrating to stress measurements taken at different times of the year.

3. UPDATED INTAKE SLOT CUTTING ANALYSIS

The slot cutting program at Mactaquac was recently updated in an effort to better optimize the timing of slot cuts in the intake. A 3D finite element model was developed and analyzed using the latest version of GROW3D running in ANSYS. It is noted that during the course of the updated model calibration, the concrete growth law was changed to allow a larger concrete growth rate in the direction of tensile stress. The updated concrete growth law and finite element model is shown in Figure 3.

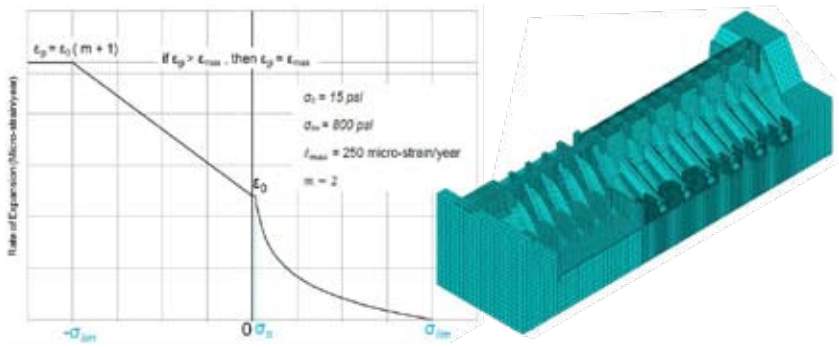

Figure 3 : (a) Update Concrete Growth Law b) Intake and Spillway FE Model

Figure 4 shows the location of the slot cuts in the water retaining structures and summary information on timing and re-cutting of the slots. The intake slots are cut down to roughly the same elevation at the floor of the intake water passage (el 60).

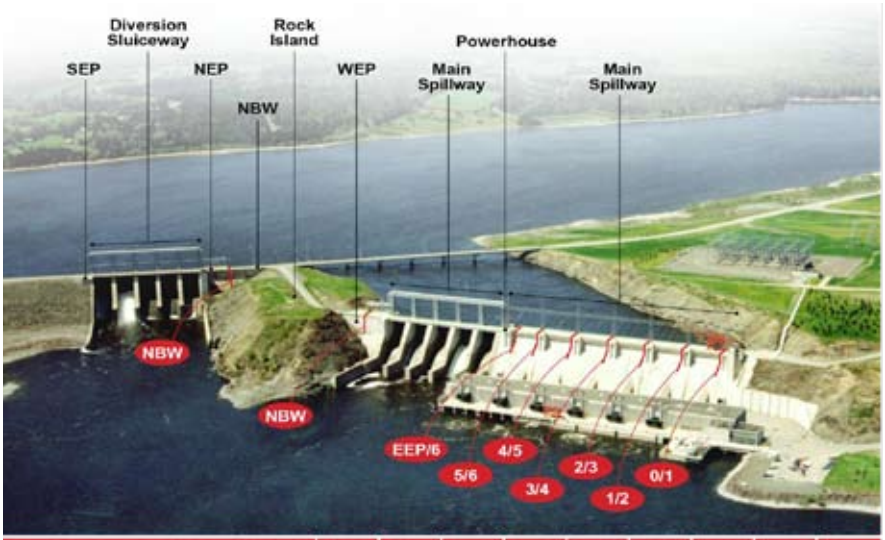

	NBW	WEP	EEP/6	5/6	4/5	3/4	2/3	1/2	0/1
Year of first cut	1993	1993	2000	1988	1989	1992	1989	1992	2015
No. of Re-cuts	8	5	2	7	5	4	6	6	0
Total sum of saw wire diameters used (mm)	146	88	45	121	99	83	111	103	30

Figure 4 : Slot Cut Locations in the Water Retaining Structures Including Cut Summaries

The geometry of the intake and spillway at Mactaquac is such that concrete expansion has a compound effect on the spillway EEP as shown in Figure 5. In the early stages of the conceptual design of remedial measures, a large strut was proposed to replace the spillway deck with a massive reinforced concrete beam. This would eliminate the need for slot cuts in the intake. However, the size of the strut was limited due to the required flood handling capability of the spillway. In addition, the strut would not stop the push from the spillway ogee into the intake Unit 6 water passage. Therefore, after considerable analysis and review, it was decided that slots should be cut in the intake and have the upper portion of the intake blocks behave independently. The design of the original slot cuts at Mactaquac in the late 1980s was undertaken using an elastic equivalent temperature model to model concrete expansion. The enhanced creep behavior of AAR affected concrete was simulated using an effective modulus approach. The model was subsequently refined to include the simulation of concrete cracking and this model predicted significant cracking of the intake water passage piers as a result of slot cutting. The intake slot cut design included the provision of post-tensioned anchors to stabilize the structure against sliding in the event that adverse cracks developed in the water passage piers.

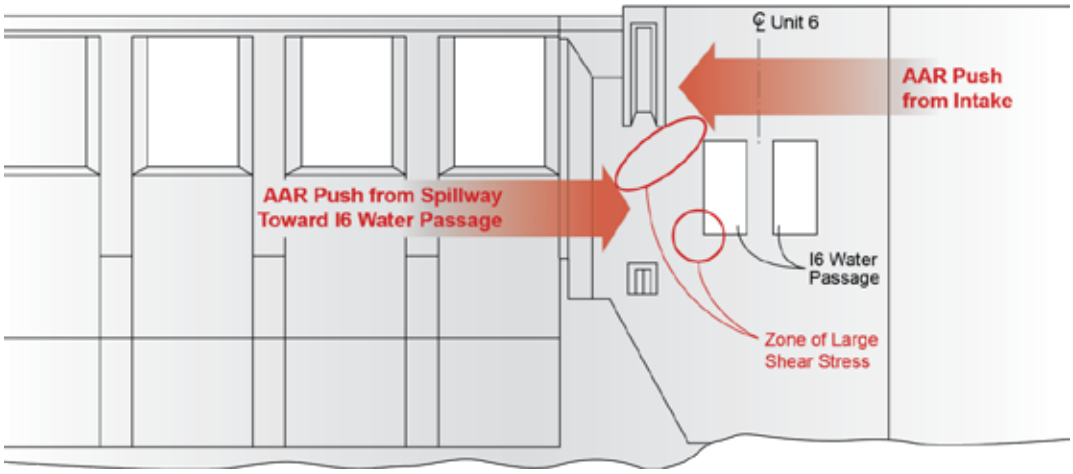

Figure 5 : Interaction Between Intake and Spillway

The updated slot cut scheme (year 2015 to 2030) for Mactaquac Intake Structures has been developed to reduce the following:

- Total number of required slots
- Movement of the intake water passage piers
- Development of the tensile and shear stresses in the intake passage piers.

The initial slot cutting schedule was developed to maintain the slot open and this was done prior to the development of GROW3D. In the current update, some sensitivity analyses were undertaken using GROW3D and it was found that the ideal time to re cut a slot was when the open width of the slot had reduced to about 2 to 5 mm at el 80 at a middle section in the plane of the intake gate slots. It should be noted that el 80 corresponds to the elevation of the ogee crest of the Main Spillway and it was also considered necessary to keep the EEP/6 slot open at this elevation. The upper portion of the slot is allowed to close for a short period of time without having a significant effect on the water passage pier deflections and stresses.

As mentioned earlier, a balanced slot cut plan is required to manage the deformations and stresses in the intake water passage piers. To illustrate this further, the slot cuts EEP/6 and 0/1 are discussed in more detail.

The pre-slot (1988) and post-slot (2010) computed longitudinal displacements of the intake are plotted in Figure 6. From Figure 6, the deflection of the spillway EEP towards the spillway has been reduced by the slot cutting program. As shown in Figure 4, the EEP/6 slot was not cut until the year 2000. The concrete growth in the main spillway rollway caused longitudinal movement of spillway concrete at and below el 80 which was directed towards the Intake 6 water passage with its floor at el 60. This movement towards Intake 6 resulted in a shear stress of about 400 psi at the base of the intake piers (as shown in Figure 7). An inspection of the Intake 6 water passage showed some initial cracking had developed as a result of these movements. Therefore a slot cut was recommended at the EEP/6 and it was installed in the year 2000. Figure 7 shows Unit 6 shear stresses were reduced considerably as a result of the EEP/6 slot cut, i.e., to around 200 psi by the year 2005. Therefore the slot achieved the desired result. It should be noted that the shear strength of AAR-affected structural elements is typically higher than normal mass concrete because the buildup of compressive stresses (restrained expansion) overcomes the tensile stresses associated with large shear stresses. This effect is discussed in more detail, and with an example, in Curtis et al (2005).

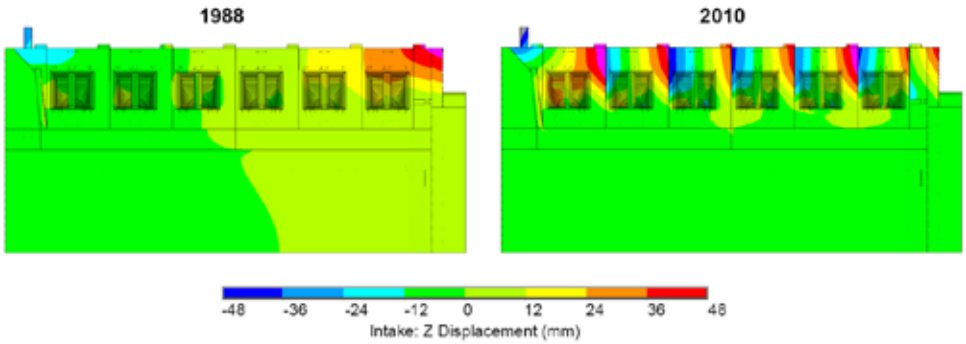

Figure 6 : Computed Longitudinal Displacements of the Intake – Looking Downstream

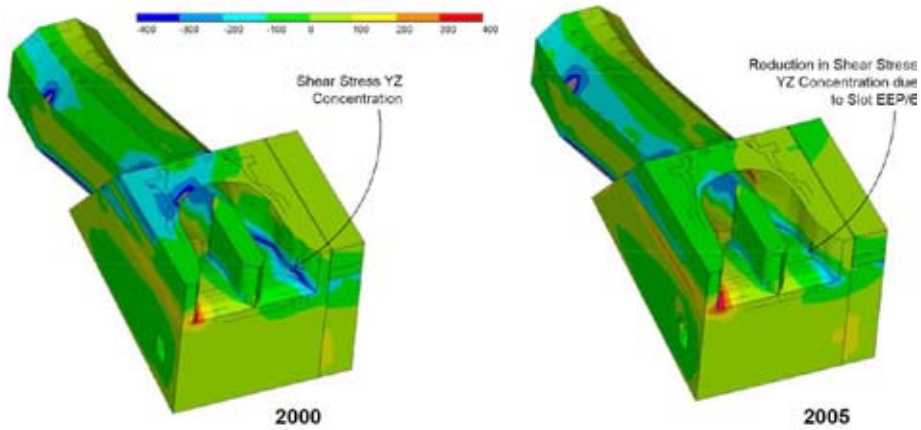

Figure 7 : Intake 6 – Computed Shear Stresses in the Water Passage

In order to illustrate the response to slot cutting, the computed and measured response at Intake 1/2 is provided. Figure 8 presents the computed slot width change for Slot 1/2 as a function of time, Figure 8a shows the computed open width and Figure 8b shows both the elongation of Intake 2 block and the slot closure at Slot 1/2. These measurements are made using invar rod extensometers in the upper gallery of the intake. The upper gallery is shown in Figure 2. From Figure 8b, the measurements and computed response is in excellent agreement.

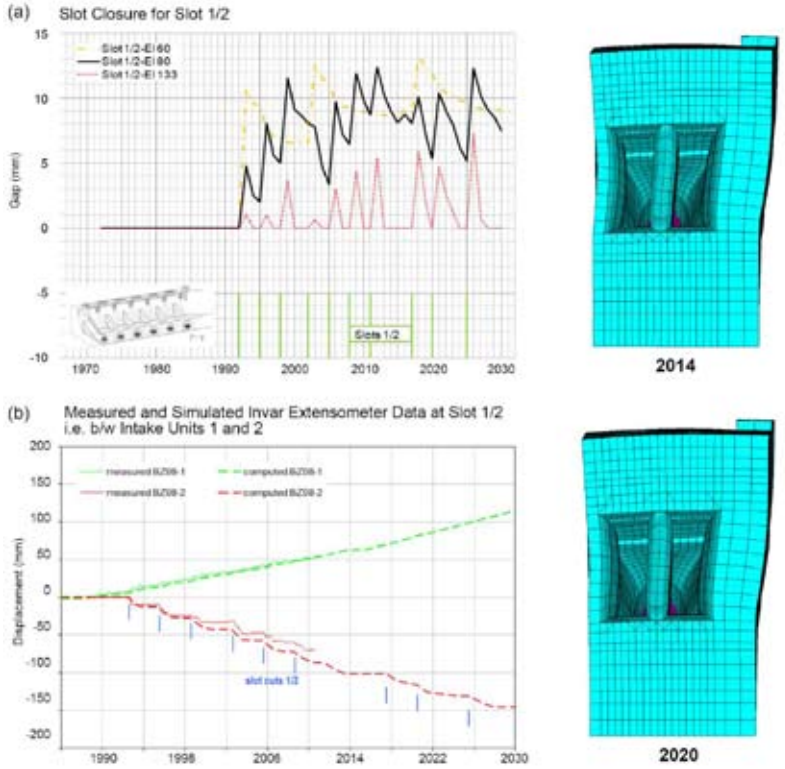

Figure 8. : (a) Computed Slot Width Versus Time (b) Measured and Computed Intake Block and Slot Closure at Slot 1/2 (Right) Deformed Shape of Intake 1 before and after 2015 Slot Cut

As indicated in Figure 4, the Intake 0/1 slot was initially cut in 2015. This was done to relieve the relatively large shear stresses that had developed in the Intake water passage piers. Figure 8 shows the deformed shape of the Unit 1 Intake block before and after the 2015 slot cut. The 0/1 slot cut caused an immediate shear stress reversal from -400 psi to 100 psi in the Unit 1 Intake piers as shown in Figure 9.

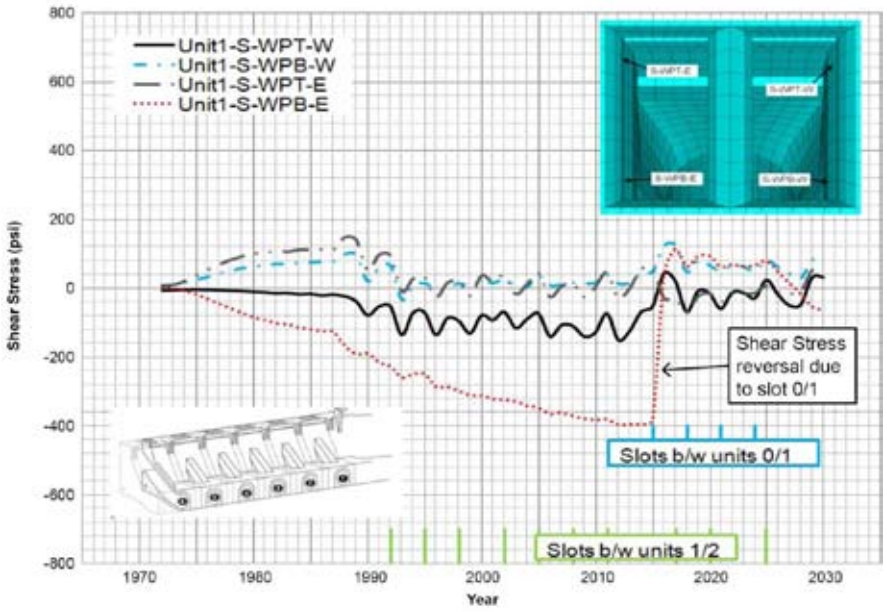

Figure 9 : Intake 1 Water Passage Shear Stresses Versus Time

4. AAR EFFECTS IN THE POWERHOUSE

The first sign of AAR-induced deformations at Mactaquac was the opening of the Line J joint at the Turbine Floor and Line F under the generator floor in the powerhouse. The locations of the Line J joint and Line F are shown in Figure 10. Figure 10 also shows some key instrumentation which will be used to illustrate the effects of differential vertical concrete expansion on behavior of the tailrace substructure. From Figure 10, invar rod Extensometer BZ-27 measures an elongation rate of 4.5 mm/yr under the generator floor and about 90% of this is directed in the downstream direction (based on other instrumentation not shown). A large portion of this downstream displacement is due to an AAR-induced "curl" of the tailrace piers.

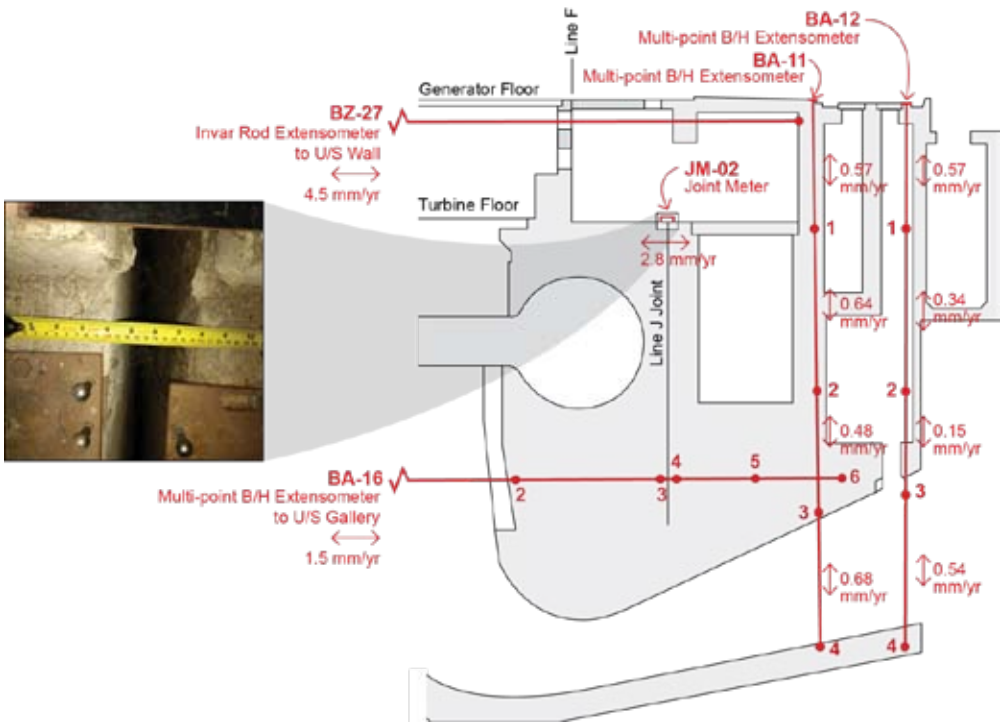

Figure 10 : Downstream Portion of Powerhouse Showing Key Instrumentation

For this review, instrumentation at Unit 2 was selected for data processing to illustrate the "curl" behavior mechanism discussed above. Figure 10 shows the selected instruments at Unit 2. From Figure 10, the multi-point Borehole Extensometers BA-11 and BA-12 measure the vertical displacement increments between anchor points in the tailrace substructure. Although the el -29 gallery is not shown in Figure 10, Borehole Extensometer BA-16 measures the elongation from the el -29 gallery (see Figure 2 to locate el -29 gallery) to just beyond BA-11. The displacement at the el -29 gallery is essentially zero due to foundation rock restraint hence BA-16 measurements at Anchor 6 represent downstream translation.

The differential expansion in each incremental height at similar elevations can be used to compute downstream deflections assuming Anchor Point 4 is the fixed end of a cantilevered column. The rotation and displacement of a cantilevered column subjected to differential expansion through its depth (d) is given by

$$\theta_B = \frac{\Delta\varepsilon \times L}{d} \quad ...(10)$$

$$\Delta_B = \frac{\Delta\varepsilon \times L^2}{2d} \quad ...(11)$$

Where

L and d are the length of cantilever beam and depth, respectively

$\Delta\varepsilon$ is the differential vertical expansion.

The accumulated horizontal downstream displacement using the extensometer data over the four vertical segments as summarized in Figure 10 is

$$\Delta_i = \Delta_{r(i-1)} \times L_i + (\theta_i \text{ x } L_i)/2 \quad ...(12)$$

Where

i is the current segment starting at the base (Anchor 4 in Figure 10)

Δ_i is the displacement at the top of the current segment

$\theta_{r(i-1)}$ is the accumulated rotation at the top of the last segment.

From Table 2, the downstream displacement rate at the tailrace deck level is 4.04 mm/yr with 1.5 mm/yr due to translation at el -25 and the remainder (2.5 mm/yr) is due to differential vertical concrete growth of the tailrace substructure. The computed 4.04 mm/yr is quite close to that measured by BZ-27 (4.5 mm/yr) shown in Figure 10. The rate of Line J joint opening is less than that measured by BA-27 because the unit block concrete around the scroll case is expanding due to AAR but the dry generator floor is not. It is of interest to note that the stresses in the tailrace piers caused by differential vertical expansion would be relatively small, and this phenomenon would be difficult to stop without causing issues elsewhere in the substructure.

A global finite element model of the powerhouse has been developed for all six units as shown in Figure 11. The model has been calibrated to a massive amount of structural and turbine/generator unit parameters data totaling more than 300+ calibration measurement items. It is of interest to note that the modified concrete growth law shown in Figure 3 was developed to improve the Intake updated slot cut model calibration and when it was applied to the powerhouse a remarkable improvement in the calibration was achieved.

Table 2 : BA-11, BA-12 and BA-16 Extensometers – D/S Deflection Caused by Differential Vertical Strain and the el -25 Translation

			BA-11			BA-12			D/S Dsp due to differential Vert Growth in Pier					Add BA-16 Translation	
Location	Total Length	Increment Length	Rate	Increment Rate	Strain Rate	Rate	Increment Rate	Strain Rate	Differential Strain	Theta	Total Theta	D/S Disp	Elev	Incremental D/S Displacement	Total D/S Dsp
	(m)	(m)	(mm/yr)	(mm/yr)	(με/yr)	(mm/yr)	(mm/yr)	(με/yr)	(με/yr)	μ-Radians	μ-Radians	(mm)	(ft)	(mm/yr)	(mm/yr)
C-1	5.95	5.95	0.57	0.57	95.8	0.57	0.57	95.8	0.0	0.000	171.111	2.64	37.0	1.02	4.04
C-2	14.30	8.35	1.21	0.64	76.6	0.91	0.34	40.7	35.9	66.667	171.111	1.63	17.5	1.15	3.02
C-3	19.75	5.45	1.69	0.48	88.1	1.06	0.15	27.5	60.6	73.333	104.444	0.48	-9.9	0.37	1.87
C-4	26.60	6.85	2.37	0.68	99.3	1.60	0.54	78.8	20.4	31.111	31.111	0.11	-27.8	BA-16 = 1.5	1.5
	Vertical Rate		5.84	Vertical Rate		4.14				0.0	0.0	0.00	-50.3		0

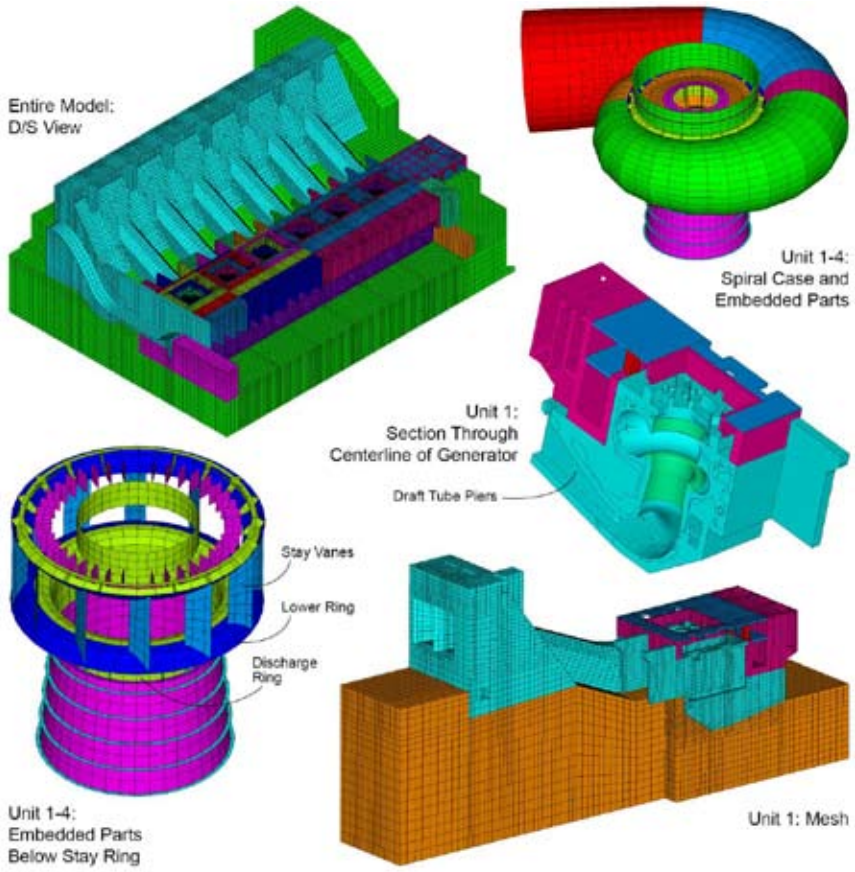

Figure 11 : Global Finite Element Model and Selected Components

Concrete growth in the powerhouse was causing the embedded turbine components to deform in an oval shape and this was affecting clearances in the cross-flow direction where the discharge ring diameter was reducing at a steady rate. This was causing issues with blade tip clearances, and extensive grinding and re-working of the units was required. Transverse slots were cut between units as shown in Figure 12. The computed response to the transverse slots is shown in Figure 13 and the improvements in the critical cross flow direction have been confirmed by measurements. As noted previously, the penstocks were cut and couplings installed from 1996 to 2001 at one unit per year. The penstock cuts improved the downstream "racking" of the turbine stay ring and reduced the stresses in the draft tube piers. However, due to space limitations the penstock cuts are not discussed further herein.

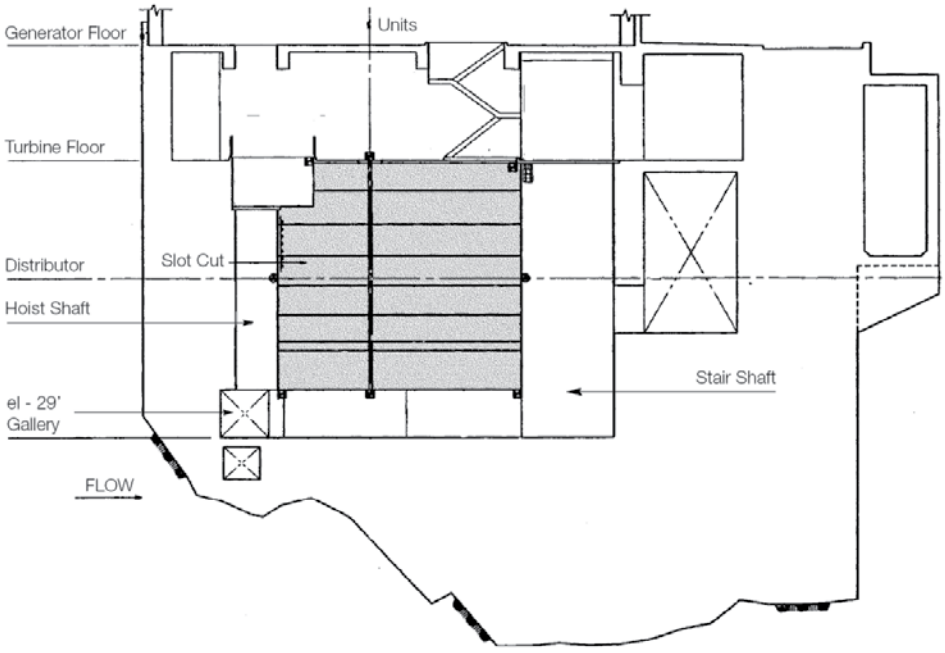

Figure 12 : Extent of Transverse Slots Between Units

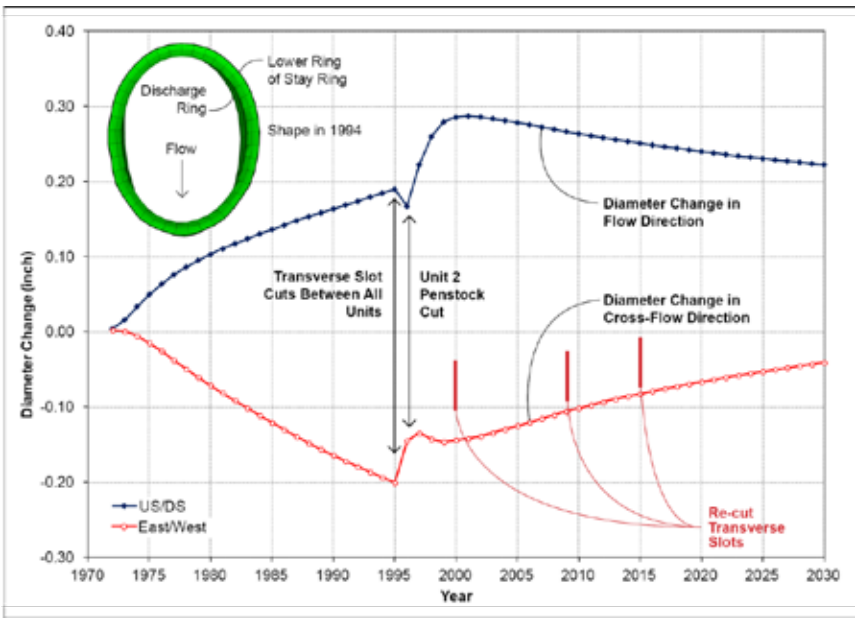

Figure 13 : Computed Response of Discharge Ring to Transverse Slots

The stresses in selected turbine stay vanes were measured in 1994 and the computed stresses from GROW3D compared well to these measurements. The location of the stay vanes is shown in Figure 11. The computed vertical stresses in 1994 and 2016 are contoured in Figure 14. The stay vane material is modeled with a non-linear stress-strain law and some yielding of the stay vanes has occurred. However, the plastic strains are well below the ultimate strain for this material. It is noted that one of the unit parameter measurements is measurement of the height change of the leading and trailing edge of the stay vanes. The model calibrated very well to these measurements therefore the computed stresses are considered to be quite realistic. There is concern for potential cracking of the stay vanes given the high stresses and their thick cross-section. It is noted that the stay vanes are stressed in a net tensile stress due to the upward pull of the concrete on the upper ring of the stay ring.

Finally, the draft tube piers are becoming highly stressed due to a downstream dipping thrust caused by restrained AAR expansion and the shear stress induced by the downstream translation of the concrete above the draft tube roof (as measured by BA-16, see Figure 10). GROW3D predicts a maximum compressive stress in the draft tube piers of about 1,800 psi. It also predicts only a small increase in stress going from the present to 2030 due to stress dependent and concrete creep effects. The stresses in the draft tube piers were measured in 1989 and the maximum principal stress was 1,200 psi compression dipping in the downstream direction. The intermediate principal stress was 700 psi compression. GROW3D matched the maximum principal stress very well but slightly underestimated the intermediate principal stress. The stress of the draft piers was checked using the procedure given by Balakrishnan and Murray (1988) and the piers were found to be acceptable to the year 2030 and beyond assuming concrete compressive strength loss of up to 25%. It is noted that concrete strength is closely monitored.

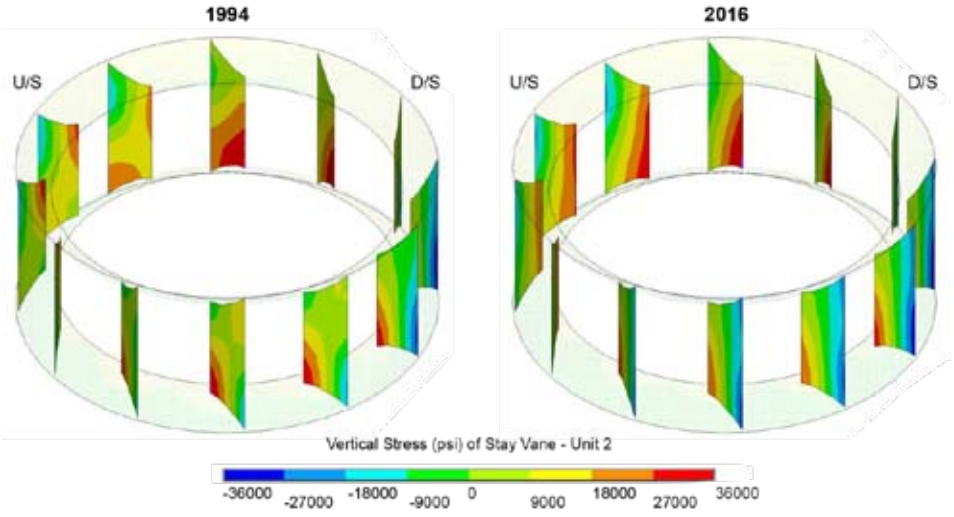

Figure 14 : Computed Vertical Stresses in Turbine Stay Vanes

5. CONCLUSIONS

The following conclusions are drawn from this work:

- The concrete expansion rates at Mactaquac are very large at about three times the rate observed at many other AAR-affected dams and powerhouses.
- Slot cuts installed in the Intake and Powerhouse are used to improve clearances for spillway gates and turbine embedded parts ovaling and unit alignment issues. The ovaling effect causes significant stressing of the embedded parts and also the inner and outer headcovers of the turbine.
- The geometry of the intake and spillway is such that alternatives to slot cutting were not available.
- The geometry of the powerhouse was such that slot cuts could be installed relatively easily between existing stairwells and hoist shafts and the benefit was immediate and ongoing.
- Small amounts of differential vertical concrete expansion can cause significant horizontal deflection of the concrete piers without causing large stresses in the piers themselves.
- The concrete growth law was modified to simulate increased concrete growth rate in the direction of tensile stresses. This modification greatly improved the GROW3D model calibration for the Intake and the Powerhouse. It is noted that there is no technical literature to support this as laboratory testing of this effect would be difficult, however the observations at Mactaquac certainly support its use. This modified growth law may be project specific, as we have not used it on any other AAR-affected projects.
- Steel stresses in the stay vanes and concrete stresses in the draft tube piers are quite large and close monitoring of these structural elements is required.
- GROW3D has proven to be a practical tool for the analysis of AAR-affected dams and powerhouses. More sophisticated scientific models exist with considerable input requirements and it is doubtful that this data would ever be available. Also, many of these scientific models do not properly account for concrete creep; hence they likely overpredict concrete stresses.
- The results of these analyses are currently being used to help update the estimate of the remaining service life of these structures.

ACKNOWLEDGEMENTS

The authors would like to thank NB Power for their permission to publish this paper. We would also like to gratefully acknowledge the diligent work and input by NB Power engineers, technicians and plant staff. In addition, we acknowledge the helpful input provided by the ongoing Independent Review Board and the past contributions of Robin Charlwood who directed the project for over 20 years from about 1985.

REFERENCES

Balakrishnan, S. and Murray, D.W., 1988. “Strength of Reinforced Concrete Panels”, Canadian Journal of Civil Engineering, Vol. 15, pp 900–911.

Charlwood, R.G., Solymar, Z.V. and Curtis, D.D., 1992. “A Review of Alkali Aggregate Reactions in Hydroelectric Plants and Dams.” Proceedings for the International Conference of Alkali-Aggregate Reactions in Hydroelectric Plants and Dams, CEA and CANCOLD, Fredericton, pp 1–29.

Codrington, J.B., May, T.H. and Curtis, D.D., 2007. “Spillway Gate Rehabilitation and Intake Bulkhead Design for Mactaquac GS.” CDA 2007 Annual Conference, St John’s, NL, Canada.

Curtis, D.D., 2000. “Analysis of the Structure Response to Recent Slot Cutting at Mactaquac Generating Station”, 11th International Conference on Alkali-Aggregate Reaction, Quebec City, QC, Canada, pp 1283–1291.

Curtis, D.D., 1995. “Modeling of AAR Affected Using the GROW3D FEA Program.” Proceedings for the Second International Conference on Alkali-Aggregate Reaction in Hydroelectric Plants and Dams, USCOLD, Chattanooga, Tennessee, pp 457–478.

Curtis, D.D., Davis, J.D., Rahman, S. and Powell, R.C., 2005. “Updated Assessment of Concrete Growth Effects on a TVA Dam”. The 25th USSD Annual Meeting and Conference was held in Salt Lake City, Utah.

Ghali, A. and Favre, R., 1994. Concrete Structures Stress and Deformations, 2nd Edition.

Thompson, G.A., Steele, R.R. and Coulson, D.M., 1995. “Management of Concrete Growth at Mactaquac Generating Station”, Proceedings for the Second International Conference on Alkali-Aggregate Reaction in Hydroelectric Plants and Dams, USCOLD, Chattanooga, Tennessee, pp147–159.

Thompson, G.A., Charlwood, R.G., Steele, R.R. and Curtis, D.D., 1994. “Mactaquac Generating Station Intake and Spillway Remedial Measures.” Proceedings for the Eighteenth International Congress on Large Dams, Durban, South Africa, Vol. 1, Q-68, R-248, pp 342–368.